We are IntechOpen, the world's leading publisher of Open Access books Built by scientists, for scientists

4,800
Open access books available

122,000
International authors and editors

135M
Downloads

Our authors are among the

154
Countries delivered to

TOP 1%
most cited scientists

12.2%
Contributors from top 500 universities

CLARIVATE ANALYTICS BOOK CITATION INDEX INDEXED

WEB OF SCIENCE™

Selection of our books indexed in the Book Citation Index in Web of Science™ Core Collection (BKCI)

Interested in publishing with us?
Contact book.department@intechopen.com

Numbers displayed above are based on latest data collected.
For more information visit www.intechopen.com

Chapter 3

Structure of the Metallic Glass and Evolution of Electronical Properties during Glass Transition in Atomic Level

HaiJun Chang

Additional information is available at the end of the chapter

http://dx.doi.org/10.5772/63676

Abstract

Metallic glass (MGs) has many unique properties such as low density, low Young's modulus, and so on. These unique physical and mechanical properties attract much attention on their application in manufacturing production. While, structural properties such as complete absence of the long-range order and most MGs are consist of equal or more than ternary constituent which complex factors make that the atomic level structure of metallic glass still have not well known by researchers. The limited methods and data sets obtained by experiment make the acknowledge in uncovering atomic structure of melt states of alloy, and the supercooled liquid about the alloy is absent as well. These messages are important to improve and increase the understanding of MGs, as we know that glasses are essentially frozen liquid made by quenching of their high-temperature melts. Computer simulation method is an useful tool to obtain structure messages of melt and the supercooled liquid. The static, dynamical properties as a function of temperature can also be investigated by ab initio MD simulation. The atomic level rearrangement consists of both local topological structure change and chemical reordering and evolution of electronic properties of the $Al_{87}Ni_7Nd_6$ and $Ca_{50}Mg_{20}Cu_{30}$ alloy during the glass transition process is investigated, and the discussion of the results is given in this chapter.

Keywords: supercooled liquid, glass transition, microstructure, electronic evolution, metallic glass, atomic structure, electronic properties

1. Introduction

For amorphous metals, the expanding application in manufacturing production makes metallic glass (MGs) attract much attention to uncovering their atomic structure. As a consequence of the complete absence of the long-range order, equal or more than ternary constituent elements and the varying chemical affinity between the constituent elements which complex factors known by researchers. Topological and chemical short-range order is existed in MGs and is the most pronounced structure factor in these amorphous alloys.

Atoms packing from micro-observation view and structural different together with changes by temperature decrease during the glass transition progress are important to explore these interesting properties of MGs. The electronic structure and the bond between paired atoms in amorphous alloy are still little reported.

The limited methods and data sets obtained by experiment make the acknowledge in uncovering atomic structure of melt states, and the supercooled liquid about the alloy is absent as well. These messages are important to obtain useful knowledge such as general structural models and fundamental principles of atom packing and the correlations of thermodynamic, kinetic and mechanical properties with the MG structures.

Computer simulation method is an useful method to obtain messages of melt and the supercooled liquid. The static, dynamical properties as a function of temperature can also be investigated by ab initio MD simulation from the obtain results together with the electronic structure, bond and electronic density of states evolution during the glass transition process [1, 2].

Using the first-principle computer simulation method, the atomic level structure of metallic glass was indicated, which is vital to understanding of the behaviour of these materials. The research was focussed on first-principle molecular dynamic simulation of the rapid solidification process of $Ca_{50}Mg_{20}Cu_{30}$ alloy [1] and the evolution of structural and electronic properties during the glass transition process of Al-Ni-Nd alloy [2].

Some theory means have used to propose the evolution of the structure of this alloy during the glass transition such as HA index method and bond-angle distribution function. The result indicates that the increasing pentagonal bipyramids ordering suppress the formation of the crystal structures during the rapid solidification processes.

Evidence for the existence of covalent bonds is provided by our research, the polyhedral local topological structures together with the chemical short- to medium-range order (SRO) structures play an important role in glass transition and also increase the glass-forming ability of these alloy. The charge density of the alloy was also given.

The static and dynamical properties of $Ca_{50}Mg_{20}Cu_{30}$ alloy and Al-Ni-Nd alloy during the rapid solidification process are investigated using ab initio MD simulations. The results we calculated agree well with the previous report of these MGs.

http://dx.doi.org/10.5772/63676

2. Part 1, atomic level structure of metallic glass

Since the unique physical and mechanical properties of the metallic glass, there has been increasing interest in developing and understanding this new family of materials. A number of experimental techniques, such as X-ray diffraction (XRD) and neutron diffraction, have been carried out to understand the structure of the metallic glass as well as modelling methods, which include Reverse Monte Carlo (RMC) and molecular dynamics (MD). These results given by researchers have more attraction and more attention on their application in manufacturing production.

Atomic level structure of metallic glass was investigated using ab initio MD simulations, and the local atomic structures of Ca-Mg-Cu and Al-Ni-Nd amorphous metallic glasses have been investigated by the pair distribution function (PDF) analysis of neutron diffraction data. The pair distribution function (PDF) is a pair correlation function to indicate that the probability of an atom is located at distance r from an average centre atom. PDF is used to characterize the structural properties of liquids and amorphous solids.

The α-β partial PDF is defined in Eq. (1)

$$g_{\alpha\beta}(r) = \frac{L^3}{N_\alpha N_\beta}\left\langle \sum_{i=1}^{N} \frac{n_{i\beta}(r)}{4\pi r^2 \Delta r} \right\rangle \tag{1}$$

where in the system of N atoms, N_α and N_β are the number of atoms of type α and type β, respectively. r is the interatomic distance between two atoms i (of type α) and j (of type β).

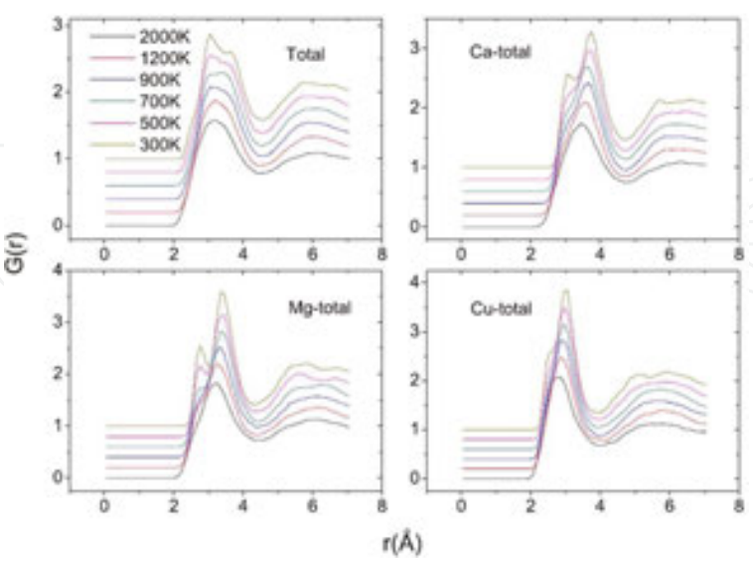

Figure 1. The total paid distribution functions and partial pair distribution functions of the $Ca_{50}Mg_{20}Cu_{30}$ alloy at different temperatures.

It can be seen that the first peak of total PDF of $Ca_{50}Mg_{20}Cu_{30}$ (**Figure 1**) gets higher as the temperature decreases, which indicates that atomic ordering in the first coordination shell increases as the temperature decreases. The first peak of total PDF starts splitting at 900 K. At the lowest temperature, 300 K, a splitting of the first peak into two peaks around 3.05A and 3.65A and a splitting of the second peak are seen. For the PDF of Ca atom, we can find a shoulder which appears at 500 K and becomes more pronounced as the temperature is decreased. This prepeak is located at 3.05A° which is equal to the interatomic distance of Ca-Cu pair and it is believed to originate from increasing interaction of the Ca-Cu atomic pairs. For Mg atom, the prepeak located at 2.75A°, which appears at 700 K, indicates that affinity of Mg and Cu atoms becomes stronger below 700 K. Besides, the shoulder of PDF of Cu atom at 300 K is due to the formation of Cu-Cu atomic pair.

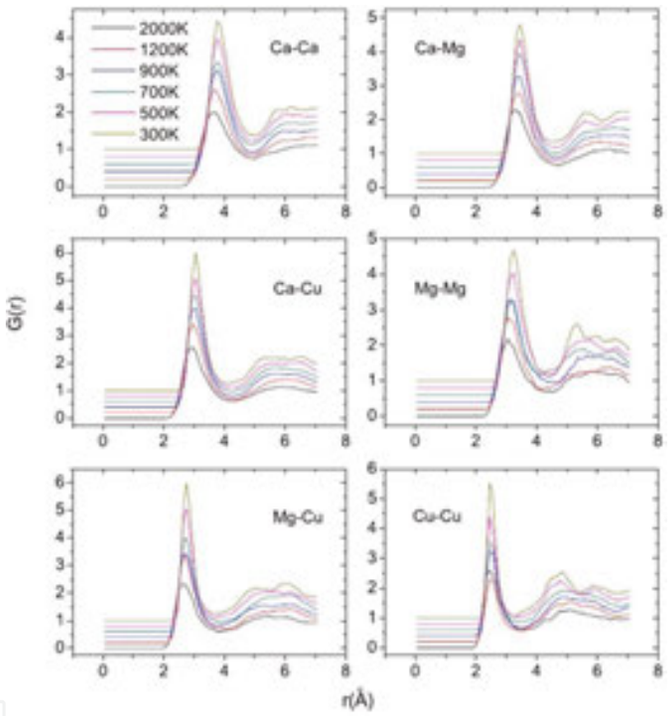

Figure 2. The partial pair distribution functions of Ca-Ca, Ca-Mg, Ca-Cu, Mg-Mg, Mg-Cu and Cu-Cu atomic pairs of the alloy at different temperatures.

The partial pair distribution functions of the different atom pairs such as Ca-Ca Mg-Mg, Mg-Cu and Cu-Cu are shown in **Figure 2**. All of these functions reveal an increase in the height of the first and second peaks with decreasing temperature, which demonstrates the increase of the short to medium range order during the solidification process, while the location of the first peak changes little at the same time. We can distinguish splittings of the second peak of all six partial pair-correlation functions. However, the splittings occur at different temperatures for these functions. For the Ca-Mg and Cu-Cu pairs, the splitting first occurs at 500 K and is well developed at 300 K. While for other pairs, the splittings occur at lower temperature than

http://dx.doi.org/10.5772/63676

500 K (the experimental Tg = 401 K) [3]. It demonstrates that some different substructures in prefer atom pairs have been formed before reaching the final glassy state.

Figure 3 shows the total PDF and partial PDF (Al-Al, Al-Ni and Al-Nd) of $A1_{87}Ni_7Nd_6$ alloy. The peaks about first and second of all the PDFs get higher during the glass transition process, which indicates that short to medium structure orderings of the associated atom increases as the temperature decreases. The increase of Ni atom PDF is obvious, which leads to the sharpness peak of the partial PDF (Ni atom) at 300 K eventually. It determines the compositional and geometrical order became stronger and formed during the glass transition process around Ni atom. Total PDF shows a splitting of the second peak at 500 K, and dislocation of the two well-developed new peaks is around 4.67 and 5.58 Å at 300 K.

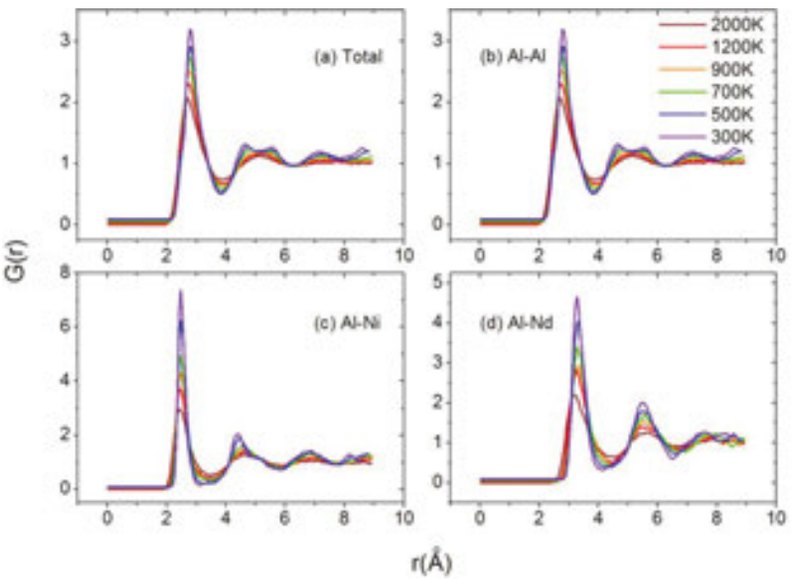

Figure 3. The total and partial pair distribution functions of the $Al_{87}Ni_7Nd_6$ alloy at different temperatures. (a) Total, (b) Al-Al, (c) Al-Ni and (d) Al-Nd.

The splitting of the second peak with the different shapes of partial PDFs may caused by the different radii of the atoms in the atomic pairs, which indicate the complex structures of the disorder systems. The partial coordination numbers of Al-Ni and Al-Nd pairs estimated from the DRP model are 10.9 and 16.4 [4]. The CNs of the Al-Nd pair decreases with decreasing temperature, which determines that Al turns to prefer to be near Ni rather than Nd atoms during the glass transition process.

3. Part 2, the evolution of structural properties during the glass transition process

Honeycutt-Andersen (HA) bond-type index is compute to obtain detailed information [5] of the local structure of the $A1_{87}Ni_7Nd_6$ alloy. Three-dimensional image of the local configurations

is given during the solidification process. The HA bond-type index represents the number and properties of common nearest neighbours of atom pair; it can used to analysis the local environment surrounding the atomic pair, which is under consideration. Each H-A bond index is classified by the relation among their neighbours with four indices of integer.

The first integer is 1 if the pair is bonded and the considered atomic pair is closer than cut-off distance or else 2. The common neighbour of the considered atomic pair is defined as the second integer, the number of bonds among common neighbours is the third number and the fourth is used to distinguish the atomic pair if the former three integers are not sufficient.

More than 12 types of the bond pairs are found in the alloy at different temperatures with the HA bond-type index method, which indicate the complex structures of the disorder systems. The variation of seven typical bond pairs of Ca-Mg-Cu alloy is shown in **Figure 4**; whereas the other pairs of 1311, 1422, 1531, 1532 and 1651 types are not shown because they are quite rare and every type of them is <2% in the whole temperature range. It can be seen that 1551 pair has a fraction of 12.5% at 2000 K and increases rapidly with temperature decreasing (41.3% at 300 K). The 1541 does not change much in the whole temperature range; the fraction of 1541 pairs at 300 K is 18.2%. These two pairs that contain five coordinated vertices represent the pentagonal bipyramids. As the melt being quenched, a large quantity of pentagonal bipyramids structures are formed in undercooled and glassy alloy. Moreover, it can be observed that the quantity of 1431 pair, which is the most popular type at 2000 K, decreases as the temperature decreases and the 1441 pair increases about 5% in the supercooled region.

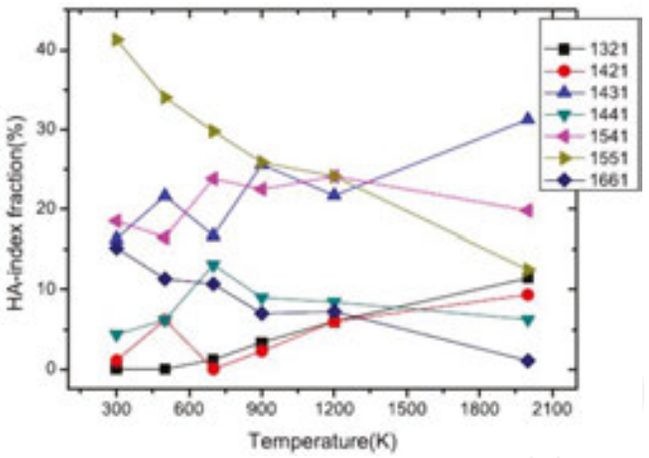

Figure 4. Evolution top seven most populated HA bond-type index in the $Ca_{50}Mg_{20}Cu_{30}$ alloy as a function of temperature.

The population of them, which indicate the fourfold bond structure, is much less than the most prevalent type of 1551 pair. In addition, the 1661 pair, which presents the sixfold bond, increases from 1.04% at 2000 K to 15.22% at 300 K. Furthermore, the 1321 pair with higher energy and larger distortion decreases obviously in the solidification process.

Much information of chemical and topological orderings of the higher order correlations can be provided by the bond-angle distribution function, which is defined about a group of three

http://dx.doi.org/10.5772/63676

atoms. One is defined as a central atom; the other two within a cut-off distance that is determined by the location of the minimum of PDF are denoted as the side atoms. The two side atoms together with the central atom define the bond angle. The bond-angle distribution function can be obtained by statistically summing the bond angles of all the groups of three atoms.

Two peaks located at about 61.8° and 101.2° at 2000 K of total bond-angle distribution about $Ca_{50}Mg_{20}Cu_{30}$ alloy (**Figure 5**), and the height of the of the first is higher. Peaks become higher during the glass transition process. The total bond-angle distribution have two peaks near 60.1°and 106.7° at 300 K. Close packing of three neighbour atoms is suggested by the first peak at around 60°, and the second peak located near 108° is consist with the pentagon configurations. The shoulder appeared at 300 K at around 145° relates to threefold coordinated atoms.

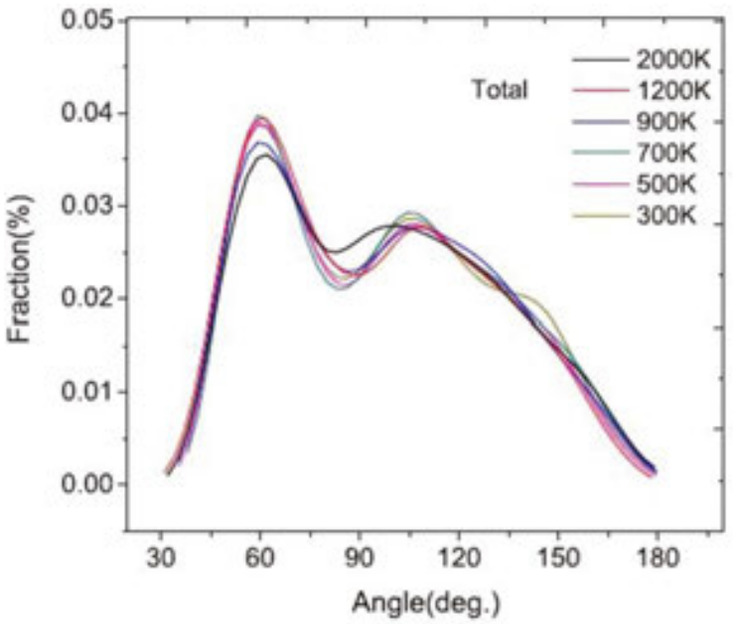

Figure 5. Calculated total bond-angle distribution functions of $Ca_{50}Mg_{20}Cu_{30}$ alloy at different temperatures.

The peaks of all the partial bond-angle distribution function of Ca-Mg-Cu alloy (**Figures 6**–**8**) become more pronounced as the temperature decreases, which exhibits that the distribution of the local structure types around the relevant atoms decreases at lower temperature. For the bond-angle distribution around Ca atoms at 300 K, predominant angles correspond to 56°, 100° and 145° can be seen clearly, and the flat peaks located at 58°, 95° and 95° are shown at 2000 K. The N-Mg-N bond-angle distribution functions in the amorphous phase (T = 300 K) have a prominent peak at 60° and 115°, while they present two broad peaks at about 60° and 109° at 2000 K. In addition, the plot of N-Cu-N shows main peaks at 60° and 110° at 2000 K, and the location of the peaks is at around 65°and 135° at 300 K. The second peak of N-Cu-N shifts to large angle during the solidification process, which is more evident than the other peaks.

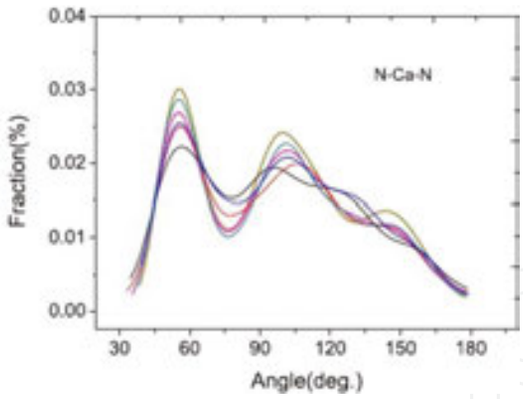

Figure 6. Calculated partial bond-angle distribution functions of the N-Ca-N (N = Ca, Mg, Cu) at different temperatures.

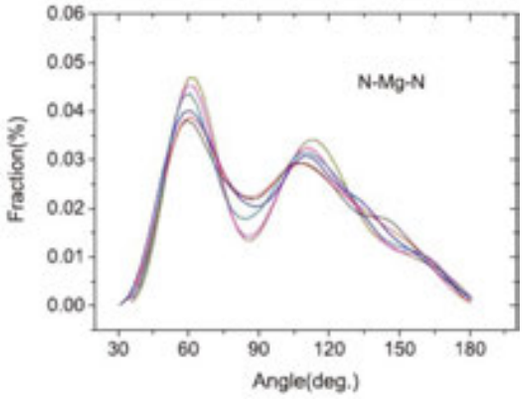

Figure 7. Calculated partial bond-angle distribution functions of the N-Mg-N (N = Ca, Mg, Cu) at different temperatures.

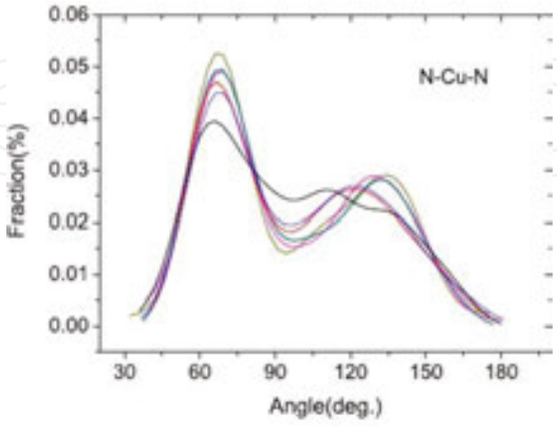

Figure 8. Calculated partial bond-angle distribution functions of the N-Cu-N (N = Ca, Mg, Cu) at different temperatures.

http://dx.doi.org/10.5772/63676

The detailed three-dimensional image information about the evolution of local atomic configuration of the Al-Ni-Nd alloy is obtained using the method of Honeycutt-Andersen (H-A) bond-type index during the glass transition process. The 1431 and 1541 bond pairs are the most two popular types seen from **Figure 9** in the molten alloy liquids, which fraction is 28 and 22%, respectively. The two pairs do not change very much in whole temperature range. Moreover, fraction of 1551 pair is 13% at 2000 K and increases with decreasing temperature rapidly which is 22% at 300 K. The 1541 and 1551 pairs represent the pentagonal bipyramids that contain five coordinated vertices. During the glass transition process, in the undercooled and glassy alloy, large number of pentagonal bipyramid structures are formed. The 1421 pair increases 5% during the rapid solidification process. Furthermore, 1311 and 1321 pairs decreases obviously, which consists with higher energy and larger distortion. The bond-type index around Al-Nd atomic pair is 1661 only, due to the large radius of Nd atom and fraction of this index is <2% during the whole temperature range.

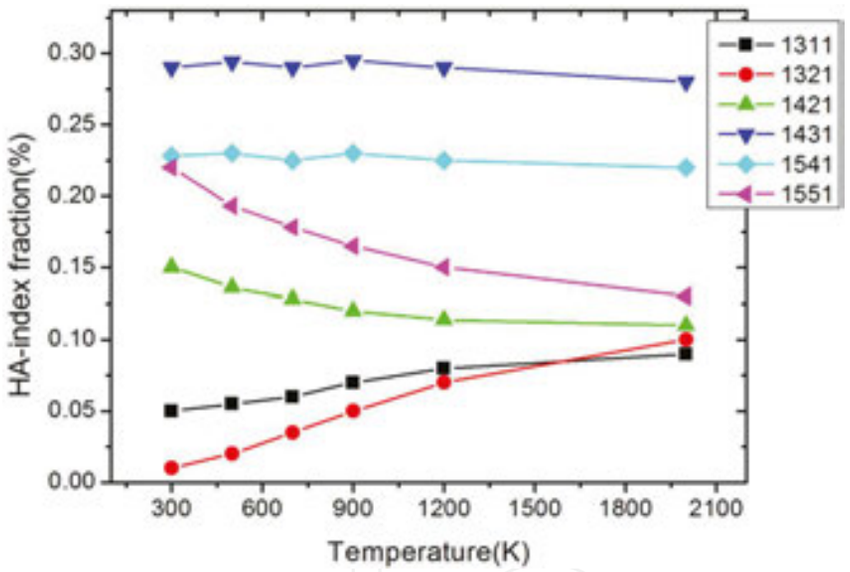

Figure 9. Evolution of the top six most popular H-A indices types in the $Al_{87}Ni_7Nd_6$ alloy as a function of temperature.

Figure 10 shows the total and partial bond-angle distributions of the Al-based alloy at different temperatures. The partial bond-angle distributions have five classes: Al-Al-Al, Ni-Al-Al, Nd-Al-Al, N-Ni-Al and N-Nd-Al (N = Al, Ni, Nd). Total bond-angle distribution exhibits two peaks at 2000 K that located at 55.48° and 106.66°, but the height of the first peak is higher. The peaks become higher by the temperature decreases. Two peaks located 56.49° and 107.79° at 300 K of the total bond-angle distribution. All the partial bond-angle distribution functions have more pronounced peaks by glass transition progress, and this shows that the distribution types of the local structure around the atomic pair decreases at low temperature. The hump between two peaks decreases as the temperature decrease and becomes less distinguishable of the Al-Al-Al, Ni-Al-Al, Nd-Al-Al and N-Ni-Al (N = Al, Ni, Nd).

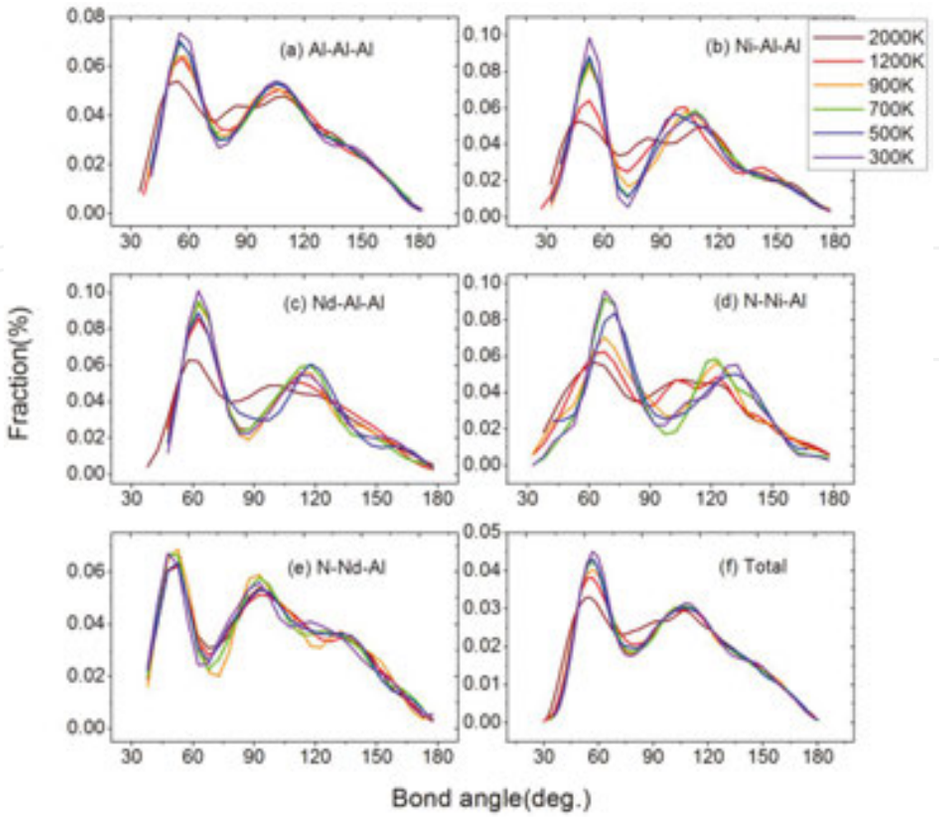

Figure 10. Calculated total and partial bond-angle distribution functions of the $Al_{87}Ni_7Nd_6$ alloy at different temperatures (N=Al, Ni, Nd). (a) Al-Al-Al, (b) Ni-Al-Al, (c) Nd-Al-Al, (d) N-Ni-Al, (e) N-Nd-Al and (f) total.

The close packing of three neighbour atoms is related to first peak at 56.49° position of the total bond angle. For Al-Al-Al, it is at around 60° shows the configuration of equilateral triangle, which is formed by the three neighbour atoms at 300 K. The second peak of the total bond angle is located near 108°, it indicates the pentagon configurations, which is agreement with the exist of the pentagonal bipyramids obtained by the HA bond-type index. The shoulder appeared at 300 K at around 145° relates to the threefold coordinated atoms. We also found that the increase in the peaks height of the bond-angle associate with the Ni is more evident than the others. The significant geometrical order around Ni is formed by the glass transition process. The shapes of the peaks for N-Nd-Al do not change very much, indicating that the neighbours' order of the elements Nd does not change much as the temperature decreases.

4. Part 3, the dynamical properties of the nucleation and glass-forming process of liquids

The dynamical properties are important for describing the nucleation and glass-forming process of liquids. The variation of mean-square displacement (MSD) as a function of temperature is also calculated through Eq. (2)

http://dx.doi.org/10.5772/63676

$$r^2(t) = \frac{1}{N}\left(\sum_{i=1}^{N}\left|r_i(t) - r_i(0)\right|^2\right) \tag{2}$$

$$\lim_{x\to\infty} \overline{r}^2 = c + 6Dt \tag{3}$$

These quantities of MSD [6] for Ca, Mg and Cu atoms are plotted in **Figure 11a–c**. The linear behaviour can be clearly seen and the slope decreases with temperature decreasing for all the three atoms. The self-diffusion coefficients, as the functions of temperature, are shown in **Figure 11d**. It is found that the self-diffusion coefficients of Ca atoms are less than the others at all temperatures, which is due to the larger radius of Ca atom. The relation between the self-diffusion coefficients and the temperature obeys an Arrhenius relationship.

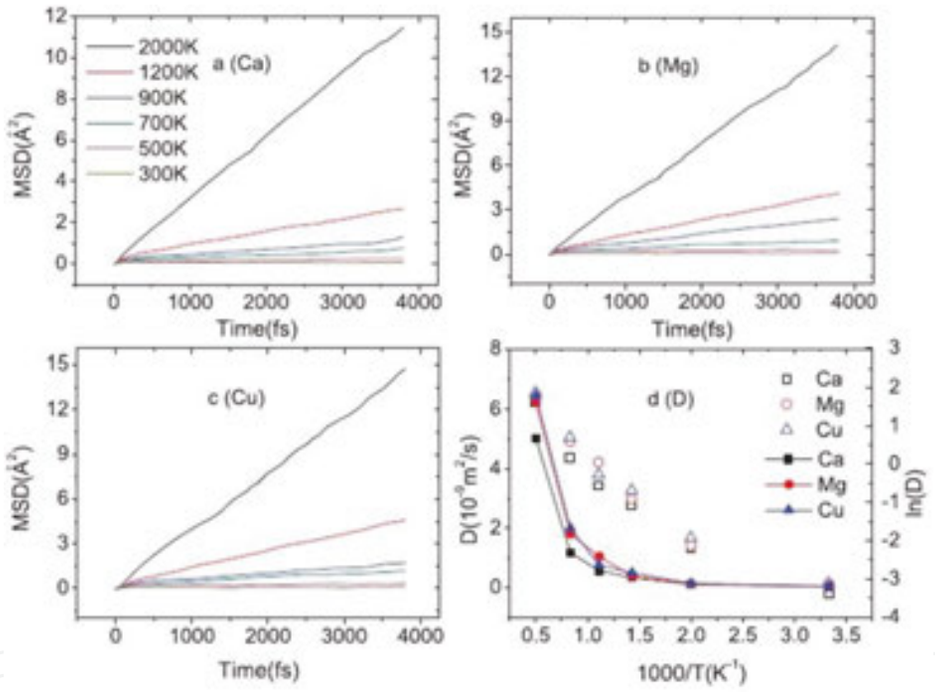

Figure 11. The MSD and self-diffusion coefficient of the alloy at different temperatures: (a)–(c) The MSD of Ca, Mg and Cu atoms; (d) variation of diffusion coefficients and the ln *D* of Ca, Mg and Cu atoms at different temperatures.

According to the Arrhenius relationship, there will be a linear relationship between the ln *D* and 1/*T*, which is also plotted in **Figure 11d**, whereas, it shows non-Arrhenius in the supercooled region in which the self-diffusion coefficients decrease more rapidly than expected. As mentioned above, the development of polyhedron local structures in the undercooled liquid delays the diffusive regime and leads to the non?Arrhenius behaviour [7], which also inhibits the crystallization and promotes the formation of the amorphous solid. The activation energy Ea is 23.01, 23.20 and 22.28 kJ/mol for the Ca, Mg and Cu self-diffusions, respectively. The pre-exponential factor D0 is 17.1210×10^{-9}, 18.9210×10^{-9} and 17.8510×10^{-9} m^2/s for Ca, Mg and Cu,

respectively. The polyhedral order and CSRO, which are enhanced in the supercooled region, decrease the self-diffusion coefficients.

5. Part 4, electronic density of states of the glass transition of the alloy

In order to investigate the electronic origin of the glass transition of the $Al_{87}Ni_7Nd_6$ alloy, we calculate the DOS for $Al_{87}Ni_7Nd_6$ alloys at different temperatures and plot in **Figure 12**. The snapshots of the configuration at 2000 and 300 K are also shown. The local DOS of N-d, Ni-d and Al-spd of **Figure 12a–c** indicates that the covalent bond is formed due to the hybridization between the electronic states of Al-p and Ni-d. Peak of DOS (Ni atom) becomes narrower and higher, the resonance between the electronic states of Ni and Al around the -2 eV is more significant during the glass transition process, shows the stronger hybridization between the electronic orbitals are formed and more ordered local structure around Ni formed. The lower peak of Nd than Ni, and the height of the peak for Nd increases slightly indicates the transition metal of Ni is more active than the rare earth of Nd during the solidification process. The chemical bonds contained in the snapshots (12 d) are calculated by the same cut-off distances of the corresponding atomic pairs at 300 and 2000 K, which presents the interaction of nearest neighbour atomic pairs are enhanced during the glass transition and the larger number of bonds are formed at the same time. It is contributing to the higher peak of DOS image (the Ni and Nd atom) at the lower temperature as well.

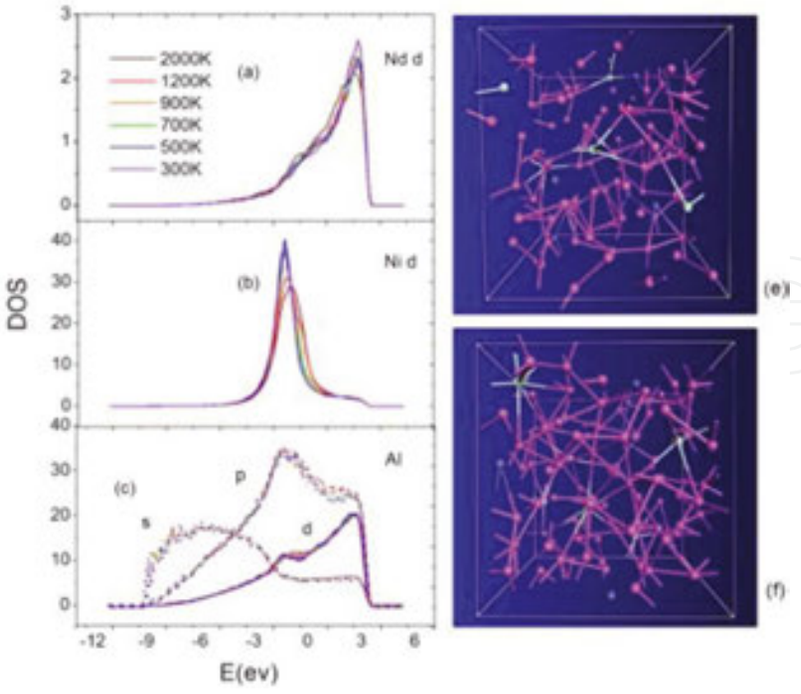

Figure 12. DOS (a)–(c) and snapshots (Al—pink, Ni—blue, Nd—green; (d) 2000 K, (e) 300 K) of the $Al_{87}Ni_7Nd_6$ alloy.

http://dx.doi.org/10.5772/63676

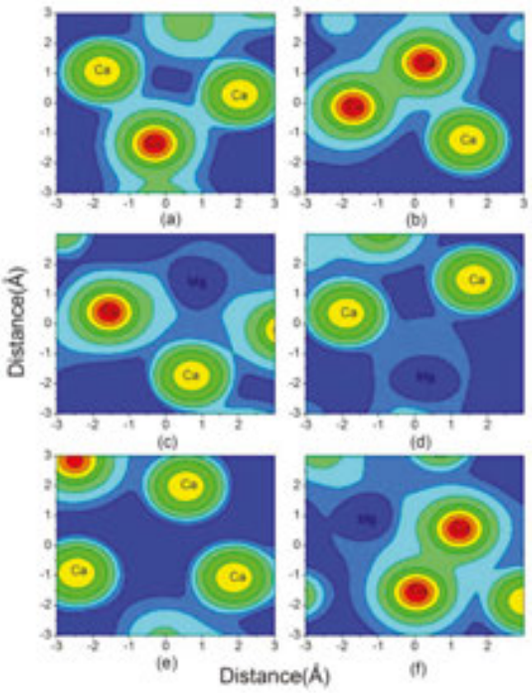

Figure 13. Contour plots of the valence electronic-charge density of amorphous solid $Ca_{50}Mg_{20}Cu_{30}$ for different atomic configurations: (a) Ca-Cu-Ca, (b) Cu-Cu-Ca, (c) Cu-Mg-Ca, (d) Ca-Mg-Ca, (e) Ca-Ca-Ca and (f) Mg-Cu-Cu.

6. Part 5, electronic charge densities of the amorphous solid

A combined neutron and x-ray diffraction study [8] have been performed for $Ca_{50}Mg_{20}Cu_{30}$ bulk metallic glass-forming system, which indicates that the average distances of Cu-Mg and Cu-Ca are consistent with the sum of covalent radii, whereas all other interatomic distances are consistent with the sum of metallic radii. Our simulation shows an accumulation of charge between Ca-Cu and Mg-Cu atomic pairs, which evidence the persistence of Ca-Cu and Mg-Cu covalent bonds (**Figure 13**). On the other hand, the covalent bonds of Cu-Cu pair are also existed as presented in the plot. The Cu-Cu interaction is not as attractive as Cu-Ca and Cu-Mg. In other words, Cu atoms prefer to cluster with Ca and Mg atoms rather than Cu itself. But this does not mean that Cu atoms repel each other. This is what the CSRO tells us. As a result, Cu-Cu covalent bonds are still found. The electrons with an sp character of the Mg atoms are transferred to the d states of Ca and Cu atoms. The accumulation of charge between Ca-Mg pairs indicates that there is Ca-Mg covalent bond in this alloy as well. While, this phenomenon is not found about Ca-Ca pair, which presents that the Ca-Ca bond is metallic bond. Our result provides string evidence for the existence of Ca-Mg, Ca-Cu, Mg-Cu and Cu-Cu covalent bonds, which is in accord with that covalent bonds between the elements dominate in the Ca-Mg-Cu alloy proposed by the former experiment. An increasing fraction of covalent bonding is benefit to increase the glass-forming ability [9], and this is in favour of the glass formation for the $Ca_{50}Mg_{20}Cu_{30}$ alloy.

7. Part 6, evolution of the electronical properties of the metallic glass

In our simulation, we also study the ground-state electronic charge densities. The charge density $\rho(r)$ in a plane defined by three neighbouring atoms at three temperatures of 2000, 700 and 300 K are plotted in **Figure 14**. The Ni ions tend to form strong interactions with Al, by the neutron diffraction data report [10], whereas the Nd bond length to Al is close to the expected sum of atomic radii about neutral ions. The accumulation of charge between Ni-Al atomic pairs at all temperatures is shown in the image 13; it indicates persistence of the Ni-Al covalent bonds. All different atomic configurations are chosen of the most nearby atomic pairs at the corresponding temperature. The interatomic distance of 2000 K is less than the others due to the broad distribution of interatomic distance at high temperature (**Figure 1**). The accumulation of charge between Al-Al atomic pair and Nd-Al atomic pair at 2000 K is more evident than the other temperature. While effect of temperature for Ni-Al atomic pair is insignificant, as a result of during the glass transition process Al atom prefer to transform near Ni atom than Al atom and Nd atom. The Al-Al and Nd-Al atomic pairs are weakly covalent bond properties in the molten liquid states, whereas Nd-Al is metallic bond properties at 300 K because of that the electronic charge density around Nd atom is a spherical distribution almost. The electrons with a sp character of the Al atom are likely transferred to the d states of Ni atoms at 300 K. The increasing fraction of covalent bond and metallic bond can increase the GFA of the alloy, and it is in favour of the glass formation during the solidification process of the multicomponent molten alloy.

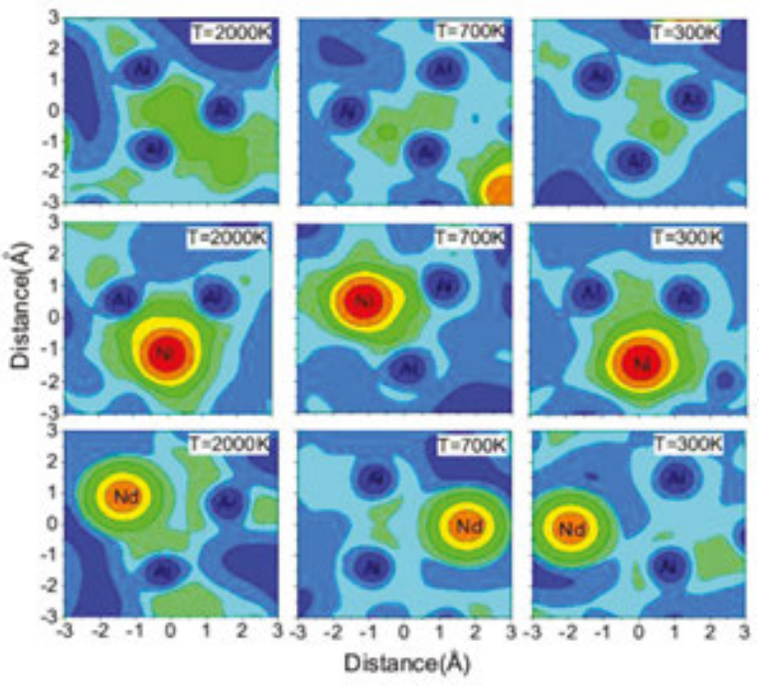

Figure 14. Contour plots of the valence electronic charge density of $Al_{87}Ni_7Nd_6$ alloy for different atomic configurations at different temperatures.

http://dx.doi.org/10.5772/63676

8. Conclusion

Ab initio molecular dynamic simulations are used to understand the evolution of structural and electronic properties during the glass transition process of the $Al_{87}Ni_7Nd_6$ and $Ca_{50}Mg_{20}Cu_{30}$ alloy based on the density functional theory. The pair correlation function, CN, diffusion coefficient, mean square displacement, HA bond-type index and bond-angle distribution at different temperatures are observed by our simulation.

The PDF images investigates that the short to medium structure orderings are enhanced with decreasing temperature during the rapid solidification process. The interaction between different atomic pairs is strengthened, and the splitting of the second peaks occurs at different temperatures for the partial PDF, which indicates that some different substructures in prefer atom pairs have been formed before reaching the final glassy state.

The CNs we calculated agree well with the previous report of Ca-Mg-Cu MGs [11]. The CN of Ca atoms changes from 14.87 to 15.39, it is from 12.15 to 12.35 for Mg atoms and it is from 9.18 to 9.32 for Cu atoms, which are very close to the previous theoretical result. According to the ECP model [12, 13], which allows the number of structural sites to be counted, each Mg atom will be surrounded by 10 Ca atoms in the binary Ca-Mg MGs, and three additional solute sites occur at the interstices of these Mg-centred clusters. The CNs around Ca atom are about 15 while which is more than result of 13 in the Ca-Mg-Zn MGs [14], which shows that the packing around Ca atoms is more efficient in the Ca-Mg-Cu alloy. The interatomic distance we obtained and the partial coordination numbers of Al-Ni and Al-Nd pairs in our simulation are consistent with the previous experimental of the neutron diffraction and theoretical results of Al-Ni-Nd alloy [10].

The pentagon configurations and the three neighbour atoms packing are the most primary short-range order in both these two alloys, which local structural order is enhanced obviously by the decreases of temperature during the glass transition progress concluded by the bond-angle distribution methods in these two alloys, which is consist with results evaluated by the Honeycutt-Andersen (H-A) bond-type index that the amount of pentagon configurations increases during the glass transition and become the primary short-range order (SRO) as temperature decreases.

Our modelling studies of multicomponent of Al-based MGs and Ca-based MGs show that the covalent bonds of Ca-Mg, Ca-Cu, Mg-Cu and Cu-Cu pairs are existed in Ca-Mg-Cu alloy and accumulation of charge between Ni-Al atomic pairs which evidences the persistence of the Ni-Al covalent bonds in Al-Ni-Nd alloy at all the temperatures.

The evolution of structural and electronic properties during the glass transition process of Al-Ni-Nd alloy is also simulated. A result of the fact is that Al turns to prefer to be near Ni than Al and Nd during the glass transition process. In the molten liquid of 2000 K, weakly covalent properties of Al-Al and Nd-Al atomic pairs are existed, while the electronic charge density around Nd is almost a spherical distribution at 300 K.

Glass-forming ability (GFA) is also another important research issue. Inoue have provide three empirical rules for BMG formation [15, 16]: which suggested that multicomponent system of

more than three elements, difference of atomic size mismatch large than 12%, and negative heat of mixing between the components atoms tends to transform to glass easily of this multicomponent alloy system. The formation of the crystal structures is suppressed by the increasing polyhedral local structures ordering and chemical SRO of covalent bonds and metallic bonds; the increasing of the electronical interaction during the rapid solidification processes plays an important role during the glass transition and increases the glass-forming ability of the Al-Ni-Nd alloy.

We also found that the electrons with a sp character of the Al atoms are more likely to transfer to the d states of the Ni atoms. The more disordered amorphous state and the optimum bonding state seem to achieve the confused compositions and multicomponent MGs with good glass-forming ability and unique mechanical properties.

Author details

HaiJun Chang

Address all correspondence to: changhaijun01@163.com

School of Materials Science and Engineering, ShangHai JiaoTong University, Shanghai, China

References

[1] H. J. Chang, L. F. Chen and X. F. Zhu, J. Phys. D: Appl. Phys. 46, 105303 (6pp) (2013).

[2] H. J. Chang, L. F. Chen, and X. F. Zhu, J. Appl. Phys. 112, 073517 (2012). doi: 10.1063/1.4757626.

[3] O. N. Senkov, D. B. Miracle, and J. M. Scott, Intermetallics. 14, 1055 (2006).

[4] Ahn K, Louca D, Poon S J and Shiflet G J 2003 J. Phys.:Condens. Matter 15 S2357–64

[5] J. D. Honeycutt and H. C. Andersen. J. Phys. Chem. 91, 4950 (1987).

[6] J. P. Hansen and I. R. McDonald, Theory of Simple Liquids (Academic, London, 1986).

[7] A. Pasturel, E. S. Tasci, M. H. F. Sluiter, and N. Jakse, Phys. Rev. B 81, 140202 (2010).

[8] E. R. Barney, A. C. Hannon, O. N. Senkov, J. M. Scott, D. B. Miracle, and R. M. Moss, Intermetallics. 19, 860–870 (2011).

[9] R. W. Cahn, P. Haasen, and E. J. Kramer, In glasses amorphous metals, edited by Weinheim (VCH, NY, 1991).

http://dx.doi.org/10.5772/63676

[10] K. Ahn, D. Louca, S. J. Poon and G. J. Shiflet. J. Phys.: Condens. Matter. 15, S2357–S2364 (2003).

[11] Ahn K, Louca D, Poon S J and Shiflet G J 2003 J. Phys.:Condens. Matter 15 S2357–64

[12] D. B. Miracle, D. Louzguine-Luzgin, L. Louzguina-Luzgina, and A. Inoue, Int. Mater. Rev. 55, 218 (2010).

[13] D. B. Miracle, Acta Mater. 54, 4317 (2006).

[14] O. N. Senkov, D. B. Miracle, E. R. Barney, A. C. Hannon, Y. Q. Cheng, and E. Ma, Phys. Rev. B 82, 104206 (2010).

[15] A. Inoue, Acta Mater. 48(1), 279 (2000).

[16] A. Inoue, Mater Trans. 36(7), 866 (1995).

IntechOpen